GEOCHRONOMETRIA 51 (2024) 192455
DOI 10.20858/geochr/192455

Available online at https://www.geochronometria.com/

AN ASSESSMENT OF OXBOW LAKES AND THEIR POTENTIAL IN RECONSTRUCTING PAST RIVER DISCHARGE: IMPLICATION TO RECONSTRUCT PAST CLIMATE IN SOUTHERN WEST BENGAL

VIBHUTI SHIVSAGER[1], DIPJYOTI BASUMATARY[1], CHANDREYEE GOSWAMI[2], MAHADEV RAWAT[3], SAURABH SINGH[4] and MANOJ K. JAISWAL[1]

[1]Department of Earth Sciences, Indian Institute of Science Education and Research (IISER), Kolkata, Mohanpur, Nadia, West Bengal, India
[2]Institute of Rock Structure and Mechanics, Prague, Czech Republic
[3]Inter-University Accelerator Centre, New Delhi, India
[4]Department of Geology, Institute of Earth and Environmental Sciences, Dr. Rammanohar Lohia Avadh University, Ayodhya, Uttar Pradesh, India

Received 25 September 2023 Accepted 19 August 2024

Abstract
For modern fluvial systems, stage height, velocity, and cross-section help estimate a river's discharge. However, understanding the amount and fluctuations of past discharges remains a challenge. The dimensions of the meander loops/oxbow lakes are directly proportional to the river's discharge and the sediment load type. Central West Bengal, India, has a complex network of numerous oxbow lakes as a remnant of the river Hooghly, a major distributary of the River Ganga. The present work revisits Schumm's classic work to estimate river discharges from the meander loops and explores a potential proxy for estimating past discharges. Thus, it is extended to reconstruct past climate using grain size data, facies analysis, and the dimension of the meander loops coupled with the luminescence chronology of oxbow lakes. The study reveals that the region received good rainfall during reported periods of intense monsoon, and the increased discharge at different time intervals has given rise to numerous oxbow lakes. The discharge values have shown considerable fluctuations, rising to 15 to 20 times the current value and very few anomalously high, even up to 250 to 300 times, left unrecorded from other archives. The study shows the preservation of systematic growth of discharges and the meander loops with climate revealing events with anomalously high (and so highly disastrous) discharges at the scale of tens of thousands of years, usually missed from other archives. Results from Ichhamati and Hooghly River meander loops in West Bengal, India, indicate a manifold increase of discharges from the current during 1–1.5 ka (known as the Medieval Warm Period); around 2.2 ka and around 3.9 ka with low or gaps of enhanced monsoon, e.g., Little Ice Age and during 2.5–3.5 ka. This is an effort to show the potential of past meander loops to be explored well for comprehensive records.

Keywords
point bars, oxbow lakes, luminescence dating, palaeo-flood, palaeo-climate

Corresponding author: M. K. Jaiswal
e-mail: manoj@iiserkol.ac.in

ISSN 1897-1695 (online), 1733-8387 (print)

1. Introduction

Climate change has recently affected the monsoon pattern across other parts of the world, including India; hence, monsoon variability has become integral to recent and past climate change studies. Instrumental and historical records can help in such a study on a decadal to centenary scale. However, one must look beyond historical/instrumental records for sedimentological archives of fluvial deposits. Fluvial archives (depositional structures) are primarily influenced by changing climate. Climatic fluctuations, such as monsoon strengthening or weakening, are recorded in sedimentary strata and structures in fluvial deposits. Varying discharge values cause a change in grain size traveling into media (river) and can produce different forms of sedimentary units. Various stages of river maturity record different erosional and depositional features. River responds to climate changes and tectonic activities; thus, a fluvial deposit preserves the signature of the past environment (Ely *et al.*, 1993; Sridhar, 2007). Each element (e.g., delta plain, flood plain, alluvial fan, terraces and oxbow lakes) of a fluvial deposit is a potential proxy to study past environment. Deltaic plains have presented a story of past sea-level fluctuations and their effect on river dynamics (Caratini *et al.*, 1994; Goswami *et al.*, 2019). Floodplain deposits help estimate the recurrence interval of flooding (Baker *et al.*, 1983). Alluvial fans and Terraces at mountain fronts archive aggradation/incision events linked with paleo-discharges and tectonic activity. Similarly, paleo-meanders or oxbow lakes are some well-distinguished features of alluvial rivers. These can be potential archives of past climate reconstruction due to the close link of their dimensions with discharge. A meandering river forms a loop due to erosion on the convex bend and deposition on the concave bend. They form due to increased discharge and thus accelerated erosion on the outer banks of a river in meandering channels. Point bars are the package of sediments deposited at the convex bends of meandering rivers. The point bars' dimensions, sediment type and structure are directly proportional to the past discharges and thus linked with past climate. The discharge and grain size of the banks of the river essentially trigger the erosion. Several morphologic characteristics of the stable alluvial channels largely depend on the type of sediment load transported by the river or, more specifically, on the ratio of suspended sediment load to bedload (Schumm, 1968). An empirical relation exists between annual discharge, channel width, wavelength of the meander loop and silt/clay proportion (Schumm, 1968) of the sediment load. The river's discharge is directly proportional to the precipitation and, thus, climate over a longer time scale. Hence, Point bars can potentially estimate paleo-discharge and, thus, past monsoonal changes over a long-term scale.

In eastern India, the southern part of the state of West Bengal is part of the Ganga-Brahmaputra Delta and its boundary with the Gondwana basin. Being a part of the great Bengal basin, it receives most of the sediments from the Himalayas. Oblique subduction of the Indian plate under the Burmese plate has given birth to a foredeep basin bounded by fold belts. River Ganga and Brahmaputra are the major rivers that have filled the basin with sediments. Several distributaries have emerged with time and drained through eastern West Bengal. This part is thus characterized by Alluvial fans, Paleochannels, floodplains, and Oxbow lakes. Southern West Bengal basin is a result of the continuous deposition of newer alluvium sediments. Fluctuating discharge with easily erodible banks and low gradient meandering rivers have numerous oxbow lakes, channel cut-offs, back swamps, and paleochannels in the complex network of fluvial systems comprising Hooghly (Bhagirathi), Bhairab-Jalangi, Mathabhanga-Churni and Icchamati rivers. The Damodar River basin is a significant catchment basin with several distributaries in the western vicinity of the Hooghly River. Draining through Proterozoic terrain, it enters into newer alluvium near Bardhhaman. The Damodar River is characterized by its substantial water volume and abundant sediments. However, over recent geological epochs, the river's velocity has been impeded by either human-made or natural factors, causing the river to bend nearly 90 degrees and form a fan along the Hooghly River.

Most of the rainfall is received from June to September in West Bengal, with an average rainfall of 1851 mm. West Bengal receives most of its precipitation from the South West Indian monsoon. Also, around 77% of annual rainfall is only during the southwest monsoon season. The state gets the highest rainfall (30%) of South West monsoon rainfall in July, while August gets 26%. Both June and September receive 22% of southwest monsoon rainfall. The fluctuation in monsoon or yearly precipitation is considerably lower at 14%. (Source: IMD report).

During the monsoon period, several weather anomalies are observed over West Bengal. These are as follows:

- Untimely and irregular onset of monsoon,
- a wide gap in precipitation frequency that led to drought situations,
- prolonged precipitation due to the long persistence of monsoon troughs causes floods,
- the slow movement of low-pressure cells, as abrupt and intense showers again cause floods,
- early withdrawal of monsoon causing drought.

All these anomalies are an integral part of monsoon weather in West Bengal that renders spatio-temporal variability. Most rivers that drain through West Bengal experience high discharge during monsoon season. Easily erodible banks, discharge fluctuations and a lower gradient in the region promote the avulsion of rivers, leaving behind paleochannels and several oxbow lakes (especially in the eastern part of West Bengal).

Palaeohydrological studies have different aspects in geological sciences. Flood frequency and paleo-flood measurements have been beneficial for flood recurrence estimation and a better understanding of flood risk management in the peninsular river. In the case of alluvial

rivers where avulsion is so frequent, slack water deposits (SWD) are scarce, which helps us understand flood frequency in Southern West Bengal. Point bars can serve as a valuable means to understand the sequence of intense discharge events, offering insights into historical monsoon patterns and, significantly, aiding in calculating past discharges for the specific region. In flood-prone areas like West Bengal, where flood management is crucial, measuring paleo-discharges becomes essential for effective flood control. Bedrock rivers are mostly favored for palaeo-discharge estimation. Alluvial rivers avulse frequently due to erosion of softer banks. Changing course poses problems in the estimation of paleo-discharge for alluvial rivers. Despite the mentioned challenges, some empirical derivations have been formulated by workers like Carlston (1965), Schumm (1968) and Dury (1976). These derivations relate discharge with the alluvial deposits' wavelength, width, and grain size.

Various lakes throughout different geographical settings in India have been used for climatic reconstructions based on the organic content in the lake sediments. In West Bengal, fertile soil and readily irrigated land make the abandoned meander loops viable for agricultural activities. Fish productivity and various bacteria have been studied here (Maitra *et al.*, 2015; Ghosh and Biswas, 2017), but attempts to utilize these lakes in climatic studies are rarely done. Point bars thus emerge as an excellent fluvial archive for the climatic and paleo-hydrological studies in such continental settings.

In the present study, oxbow lakes and point bars are used for the past discharge estimation for the proposed study area. For some sections, Paleo discharge values from the Bhagirathi and Icchamati rivers are compared with modern discharge values, and comparing values (within range) enabled us to go further into the past discharge estimations for the rest of the point bars. This study aims to present point bars as a potential tool to address a range of questions like the recurrence of past floods, calculation of paleo discharge, reconstruction of past monsoons and to study how fluvial systems have responded to different climatic events in the past.

This article aims to address the following:

1) Verification and thus establishment of the meander loops as a proxy of past discharge estimation in the study area.
2) Utilising the point bars in monsoonal reconstruction in the study area.
3) To investigate the possibility of having information on Flood frequency (recurrence of high discharge).
4) Understand the Late Quaternary fluvial evolution of the southern West Bengal around the study area.

2. Geology and geomorphology of the study area

The study area falls under the newer alluvium of the Bengal basin. On the western side, it is bordered by older alluvium and Pleistocene lateritic sediments **(Fig. 1)**. Different fault-controlled features mark the Bengal basin's perimeter except the region close to the Bay of Bengal, where rivers drain into it. Chittagong-Tripura Fold Belt (CTFB) borders the Bengal basin in the south-eastern margin and flanks the western fringe of the Indo-Myanmar Ranges. North of the CTFB is associated with an active subsiding basin called Sylhet trough, which accommodates around 16 to 18 km of Neogene sediments. Shillong plateau, belonging to Precambrian, surrounds the Bengal basin from the north and marks the north-western boundary of the Chittagong-Tripura basin.

The Bengal Basin's geometry is uneven, with a thinner (~5 km) (Supriya, 1966), gently sloping sediment cover in the western and northern part that thickens as it moves towards the southeast (Alam *et al.*, 2003). The stratigraphy varies greatly in different regions, reflecting differences in pattern and deposition history in individual basins. Considering this, we believe the entire basin should be divided into three smaller sub-basins: (1) Northern Sub-basin, (2) Western Sub-basin, and (3) South-eastern Sub-basin.

On the eastern rim of the Indian Shield, the Bengal Basin is an asymmetric polycyclic tectonic basin. The study area is currently drained by a complex network of different river systems, forming a vast alluvial plane marked by

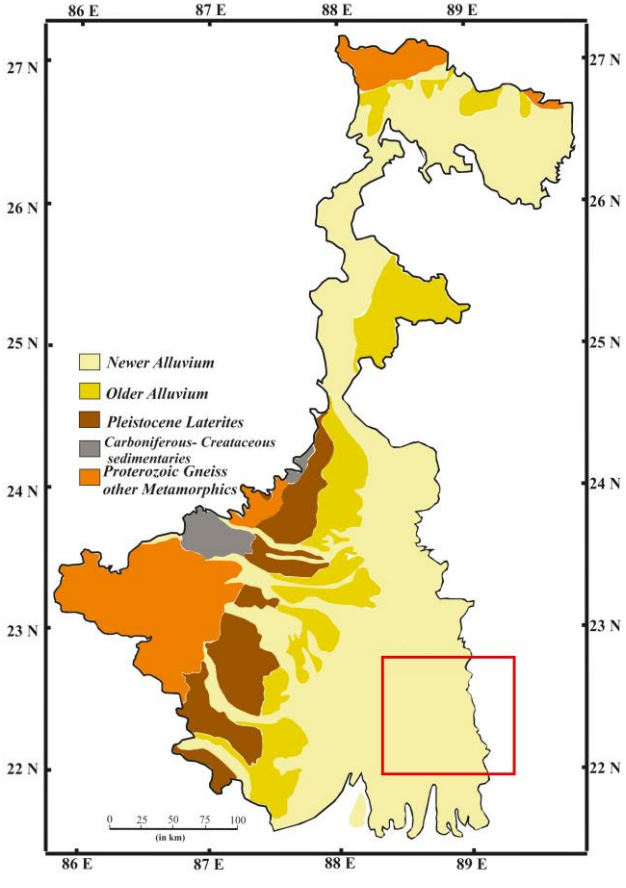

Fig. 1. *Stratigraphic map of West Bengal and the study area in the inset.*

floodplains and beautiful channel remnants in the form of oxbow lakes **(Fig. 2)**. For the present study, we have considered two systems here and these are as follows.

2.1 Bhagirathi-Hooghly River system

At Mithipur (near Jangipur) in Murshidabad district, some 40 km downstream of Farakka, the Ganga splits into two large branches, the Bhagirathi and the Padma (see **Supplementary Figure 1**). The Padma carries the main flow southeastward for roughly 90 kilometers along the Indo-Bangladesh border, leaving Indian territory beyond Jalangi, the last hamlet on the Indo-Bangladesh border. It flows roughly 132 kilometers eastward through Bangladesh before joining the Brahmaputra or Jamuna. The river continues for 115 kilometers southeast before meeting the Meghna further downstream and eventually emptying into the Bay of Bengal. Hooghly River originated at Farakka Barrage, where the Ganges bifurcate into Hooghly. It travels through the Holocene sediments of eastern west Bengal, and after traveling about ~350 kms, it debouches into the Bay of Bengal near Gangasagar island in South 24 Paragana.

2.2 Ichhamati and Jamuna River

The river Mathabhanga, which rises on the right bank of the Padma at Munsigunj in the district of Kusthia Bangladesh, splits into two branches near Majdia in the district of Nadia (West Bengal), namely the river Ichhamati and the river Churni. River Ichhamati flows for roughly 216 km until emptying into the Kalindi near Hasnabad in the district of North 24 Parganas and ultimately finds its way into the Bay of Bengal near Moore Island. River Ichhamati departs from Majdia and travels 20 km across India before crossing into Bangladesh near Mubarakpur. It travels 35 km within Bangladesh and then returns to India at Duttaphulia in the district of Nadia.

Jamuna River is a river connecting Hooghly to Ichhamati. The extensive sedimentation resulted in the formation of a channel bar in the Hooghly at Tribeni. The southward flow of the Hooghly River was obstructed, and the river was compelled to open a new outlet along the Jamuna. (Rudra, 2014). Different amounts of sediment load and discharge have caused rivers to shape themselves into different forms. A varying degree of sinuosity can be observed for different rivers. The system of interest for this

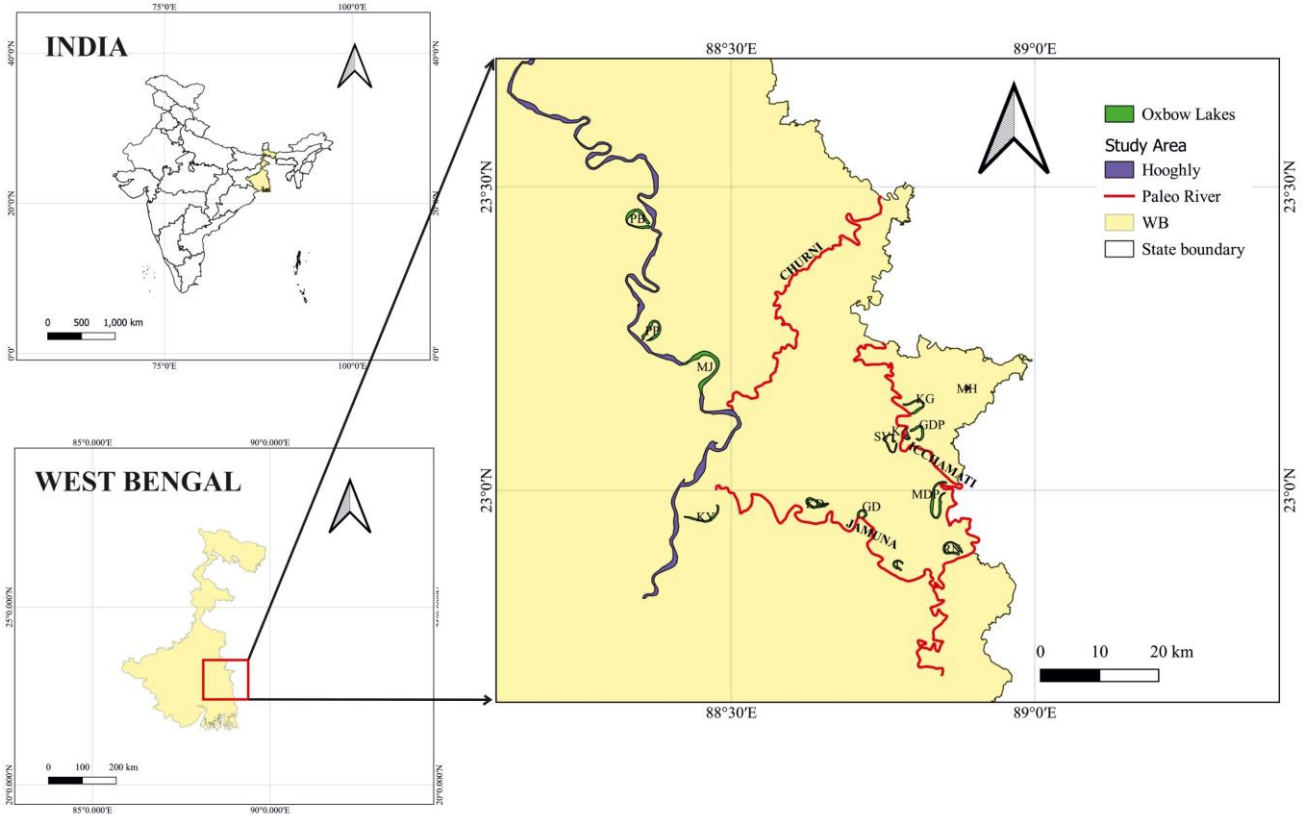

Fig. 2. *Study area map showing significant rivers, geomorphic features and oxbow lakes.*

study is highly complex as several rivers flow close to each other, producing a complex mixed system of oxbow lakes.

3. Materials and methods

Current work includes an outcome of both field- and remote-sensing-based studies of oxbow lakes and point bars; these fluvial archives are first examined through satellite imagery and then followed by an extensive field study. Processing satellite images through ArcGIS software was used for preliminary studies to identify the meander loops, and then field explorations were carried out to verify and select the sampling sites. Sixteen (16) trenches were made from different places of Nadia, North 24 Pargana and Purba Bardhhaman districts (Lat-long in **Table 1**) for appropriate sampling and then using Luminescence dating, the chronology was established along with grain size analysis of the collected samples from the selected sections. The locations were chosen to cover three different river subsystems of the Ganges. The approach toward analysis is as follows.

3.1 Field survey, Remote sensing and sedimentary analysis

The sentinel-2 satellite images of the study area were acquired from https://earthexplorer.usgs.gov/ and with the help of band combination by false color composition (FCC). Satellite imagery in false color (FCC) employs a visual representation that brings to light or improves the visibility of features that might be imperceptible or faint to the human eye. Essentially, a false-color composite involves interpreting multispectral images within the conventional visual RGB band range comprising red, green, and blue. All the oxbow lakes are traced in ArcGIS software as they have high moisture content and are pounded with standing water. After tracing all oxbow lakes, the meander wavelength, width, and radius were measured using Google Earth Pro and ArcGIS software, followed by field validation. Google Earth Pro was used to trace the Hooghly River as this river is not traceable with sentinel satellite images. Trenches were made on the point bar to construct the lithology and collect the samples for Luminescence Dating. Sedimentary Litho-columns were prepared to document the structures and preserved facies in the point bars associated with oxbow lakes. A general trend of facies for point bars was fining upward. Facies analysis helps in the differentiation of energy variation.

Table 1. *Table showing latitude-longitude and abbreviations for the sampled oxbow lakes.*

Sr No.	Location Name	Abbreviation	Lat, Long	
1	Mauja	MJ	23°11.979'N,	88°28.477'E
2	Kola	KA	23°12.957'N,	88°51.743'E
3	Santipur	SP	23°4.914'N,	88°46.471'E
4	Purbasthali	PB	23°26.858'N,	88°19.829'E
5	Panpara	PP	23°16.236'N,	88°22.826'E
6	Savaipur	SV	23°6.225'N,	88°48.520'E
7	Mahaebpur	MDP	23°5.373'N,	88°47.034'E
8	Manigram-I	KG	23°8.209'N,	88°48.729'E
9	Gadadharpur	GDP	23°5.373'N,	88°47.034'E
10	Tengra	T	22°57.872'N,	88°42.837'E
11	Ramnagar	RN	22°54.573'N,	88°51.280'E
12	Gobardanga	GD	22°52.826'N,	88°46.188'E
13	Kastadanga	KD	22°58.942'N,	88°37.646'E
14	Manigram-II	MG	23°5.322'N,	88°48.190'E
15	Mollahati	MH	23°6.436'N,	88°46.036'E
16	Kalyani	KY	22°56.176'N,	88°29.242'E

3.2 Grain size analysis

For grain size analysis, 50 g of the sample was treated with 1N HCl and 30% H_2O_2 to remove carbonates and organics, respectively. The grain size fractions were measured by a Mastersizer 3000 grain analyzer using the laser diffraction technique to measure the particle size and distribution. The intensity of light scattered as a laser beam travels through a dispersed particle sample is measured. The Mastersizer comprises three units: the optical unit, the dispersion unit, and the measurement cell unit. In basic terms, the optical unit is designed to pass red laser light and blue light through a sample, utilizing detectors to collect data on the light scattering pattern induced by particles in the sample. In our specific case, water served as the dispersion medium, and the sample was directed between measurement windows in the cell, allowing the laser to pass through for measurement purposes.

3.3 Luminescence dating

Optically Stimulated Luminescence (OSL) dates the event of daylight exposure of the sediment before burial. It relies upon the fact that the geological luminescence signal of the sediment is reduced to a near-zero residual due to exposure to daylight during weathering and transport (Aitken, 1985). "Zeroing" of such a geological luminescence signal for aeolian sediments is often easily achieved because of the availability of an unattenuated daylight flux and long transport duration. This may or may not be achieved well for fluvial sediments due to the depth of the water column, turbulence and sediment load attenuating the daylight spectrum. In total, 25 samples for OSL dating were taken in galvanized iron pipes from fluvial archives (Oxbow lakes) from Nadia, Purba Barddhaman, and North 24 Pargana districts of West Bengal. All the dating processes were carried out in restrained red light conditions. The outer 2.5 cm thick sediment was scraped off (because of chances of light exposure) and used to analyze radioactive elemental concentration (uranium, thorium, and potassium) to calculate dose rates. The middle light unexposed part was processed to extract quartz and feldspar minerals for luminescence output. This part was first treated with 1 N Hydrochloric acid (HCl) followed by 30% H_2O_2 to remove carbonates and organic matter. The required grain size fraction (90–150 μm) was sieved from the bulk sample. Quartz and feldspar grains were separated using

sodium polytungstate solution (ρ = 2.58 g/cm^3). The desired quartz grains obtained were etched with 40% hydrofluoric acid (HF) for nearly 80 min to remove the alpha dose affected layer (~10 μm) and then treated with 37% HCl for nearly 30 min to remove fluorides formed in this reaction. The final quartz grains obtained were then mounted on stainless steel cups as a monolayer using Silkospray™ silicone oil. Luminescence measurements were made on the Lexsyg smart device and the Lexsyg research device from Freiberg, Germany, fixed with blue LED arrays of wavelength 458 ± 10 nm (power = 100 mW/cm^2) and 90Sr/90Y beta source delivering a dose rate 0.15 Gy/s and 0.03 Gy/s, respectively. The luminescence purity of quartz was confirmed by the absence of sensitivity to infrared stimulation. Tests such as pre-heat plateau and dose recovery were performed to assess the optimum pre-heat temperature and test dose (Murray and Wintle, 2000; 2003). The equivalent dose (ED) was estimated using the single aliquot regenerative dose (SAR) technique following Murray and Wintle (2000; 2003) by preheating at 220°C for 20 s after applying dose recovery and preheat plateau test (**Fig. 3**). Aliquots having recuperation less than 5%, test dose error less than 20% and recycling ratio within 10% of the unity were selected for calculating the EDs. In most samples, quartz showed varying sensitivities ranging from ~900 cts/Gy/mg to ~5000 cts/Gy/mg. The shine-down curve (**Fig. 3**) decays exponentially with time, comprising fast-bleaching and slow-bleaching components. Observing the very young ages of the samples, linear fitting of the growth curve was found to be most suitable (**Fig. 3**). Dose rates of the samples were determined by using the Uranium, Thorium, and Potassium concentrations of the sediments determined by Inductively coupled Mass Spectrometer (ICPMS) and X-ray fluorescence (XRF) and uDose dosimeter instruments. Final dose rate calculations were calculated using DRAC online software (Durcan *et al.*, 2015).

3.3 Calculation of Past Annual Discharge (Paleo discharge)

A field survey was conducted to obtain samples for OSL dating and grain size analysis. Following a noble work done by Schumm (1968). Schumm conducted a study in which he sampled 33 rivers or river segments in the Midwestern United States. He created a plot correlating the silt + clay proportion with wavelength and annual discharge. His findings revealed a noteworthy impact of the silt and clay proportion on the wavelength of meandering rivers. Through multiple regressions on the collected data, he derived an equation that establishes the interrelation among wavelength (l), annual discharge (Q_{ma}), and silt + clay proportions (M). The equation is as follows:

$$l = 1890 \cdot {Q_{ma}^{0.34}}/{M^{0.74}} \quad \text{(Schumm, 1968) (1)}$$

Carlston's formula gave discharge values with huge variations from known or compared values. We also found that including silt and clay fractions in Schumm's formula has impacted the formula's accuracy to a fair extent. Schumm modified the previously available equation of Carlston (1965) with the notion that silt clay proportion must be inducted in the formula.

$$Q = \left({L}/{106.1}\right)^{2.18} \quad \text{(Carlston, 1965) (2)}$$

We needed two parameters for using Schumm's formula in the present study: Wavelength (l), and Silt+Clay fraction (M). Dimensions of oxbow lakes (l) were calculated from satellite imageries and cross-verified during field studies, and the Silt+Clay fraction was estimated from grain size analysis done using Mastersizer 3000.

Paleo discharges were estimated using the values of l and M in Shumm **Eq. 1** and **Eq. 2** above.

4. Results and Discussion

4.1 Grain size analysis

Grain size analysis was carried out to acquire the Silt and Clay fraction from the sediments to calculate paleodischarge using the Schumm formula. It has also assisted us in knowing the coarser fraction of deposits and in sensing any grain size variation at places where it was difficult to identify by the naked eye. **Table 2** has all the values for different sampled oxbow lakes. Bivariate plots (**Fig. 4**) show the data spread and help in interpreting the data.

Table 2. *Grain size analysis with Mean size (Mz), Skewness (SK), and Kurtosis (KG) of the sand samples collected from various point bars.*

Sr. No.	Sample	Mean Size (Mz in phi)	Skewness (SK)	Kurtosis (KG)
1	MJ	2.73–3.68	–0.13–0.23	1.11–1.64
2	KA	3.47–4.05	0.26–0.29	1.08–1.31
3	SP	2.17–3.80	0.14–0.22	0.27–1.66
4	PB	2.16–4.33	0.18–0.24	1.08–1.32
5	PP	4.95–5.60	0.17–0.20	0.98–1.04
6	SV	3.42–3.77	0.04–0.17	1.12–1.32
7	MDP	4.32–4.96	0.22–0.33	0.99–1.13
8	KG	4.47–6.05	0.12–0.22	0.96–1.12
9	GDP	4.25–5.84	0.15–0.22	0.95–1.22
10	T	5.44–7.00	–0.21–0.13	1.00–1.06
11	KP	2.40–4.18	0.04–0.17	0.99–1.11
12	GD	2.16–2.43	0.06–0.36	1.04–1.53
13	KD	3.04–4.80	0.05–0.13	1.04–1.54
14	MG	3.33–4.04	0.23–0.28	1.09–1.46
15	MH	5.19–6.26	0.07–0.25	0.95–1.06
16	KY	3.72–5.03	0.07–0.24	1.07–1.26

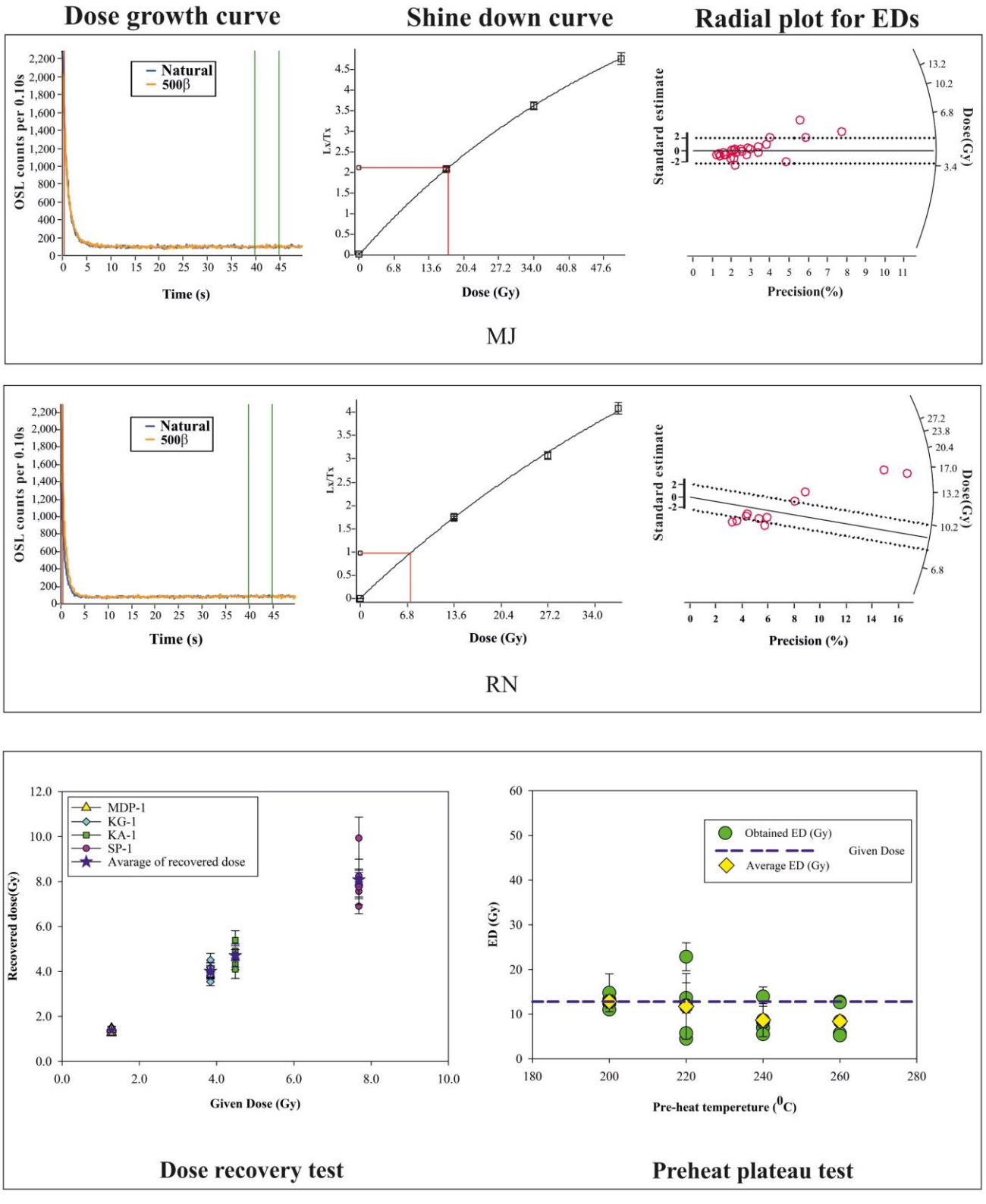

Fig. 3. *Shine down curve, Dose growth curve and histogram distribution for EDs obtained from samples.*

Three sets of oxbow lakes have been plotted in the figure where triangle, square and Circle refer to the oxbow lakes of Hooghly, Icchamati and Jamuna. It is to be kept in mind that these three rivers are eventually sub-systems of the Ganges River. Oxbow lakes ***MJ, PB, PP, and KY*** are grouped for Hooghly River; oxbow lakes ***KA, SP, SV, MDP, KG, GDP, MG, and MH*** are grouped for Ichhamati River and oxbow lakes ***KG, T, GD, KD*** are grouped for Jamuna river.

Grain size in weight percentile is plotted against the phi size of sediment distribution. The phi size is calculated using the Krumbien (1938) formula. Different phi values were obtained from different percentiles of the area falling under the curve for grain size distribution. (e.g. 5th percentile,16th percentile, 50th percentile, 84th percentile, 95th percentile). Mean size, kurtosis, and Skewness are then calculated following Folk and Ward's (1957) formulas.

Mean size and Kurtosis have been plotted in **Fig. 4a**, which shows that most oxbow lakes show leptokurtic kurtosis variation. Griffiths (1967) explained that both mean grain size and sorting are hydraulically controlled so that the best-sorted sediments have a mean size in the acceptable sand size range in all sedimentary environments. **Fig. 4b** represents a plot between Mean size and Skewness and shows that most oxbow lakes are positively skewed except a few from Jamuna River's oxbow lake. Positively skewed sediments represent mixtures of sediments from streams and surface runoffs. **Fig. 4c** shows the inter-relationship of Mean size and Sorting; we infer from the plot that dominantly oxbow lakes represent poorly sorted sediments, characteristic of rivers near the deltaic region.

4.2 River discharge estimations

Several meander loops were chosen for investigation from different subsystems of the Ganges viz—Hooghly (Bhagirathi), Ichhamati, and Jamuna to know how discharge varied through time in these rivers. Three different oxbow lakes, namely Panpara (PP), Manigram (MG), and Gobardanga (GD), which have recently been abandoned or are about to get detached from the main channel, were picked to investigate the applicability of Schumm's formula using based on (**Eq. 1**) and estimated parameter and comparing them against available annual discharge values. The annual discharge values were calculated and matched (with some range of error) with the available discharge values. **(Table 3)**. For the verification process, the Hooghly River discharge values were used from the values estimated by Rudra, (2014) and for Ichhamati and Jamuna River from Ismail Mondal *et al.*, 2016 **(Table 3)**. The upper limits of discharge for Jamuna River have been capped by being a tributary of Ichhamati River; the tributary, i.e., Jamuna River, cannot exceed the maximum discharge of the mainstem Ichhamati River.

Initially, both formulas (Schumm and Carlston) were used for discharge calculations. Still, comparing the discharges calculated using Schumm (1968) and Carlston (1965), we found that calculated discharge values fall close

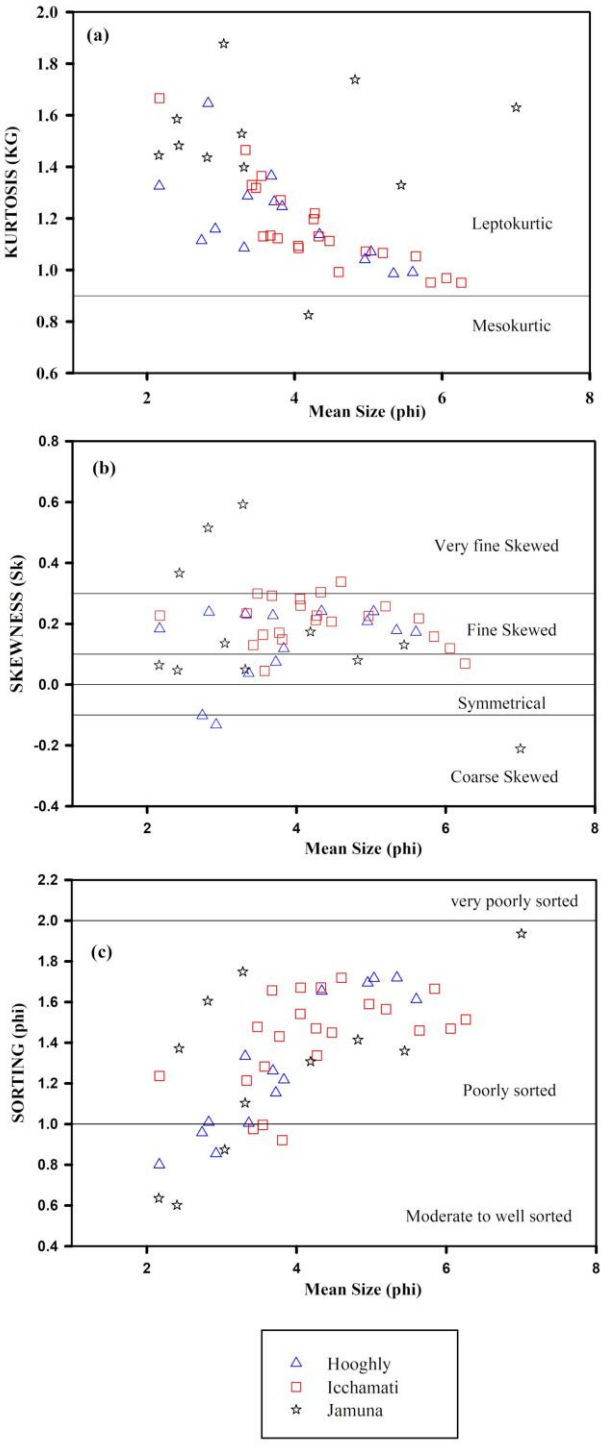

Fig. 4. *Bivariate plots showing the nature of the distribution of grain size, skewness and kurtosis.*

to Schumm's formula rather than Carlston's, which let us conclude that including Silt and clay proportion in the calculation is necessary. The Carlston formula is applicable where silt and clay proportion are not the dominant grain size component of sediments.

Table 3. *Various parameters of meander loops along with luminescence ages and calculated discharges as provided by Schumn (1968) and Carlston (1965), respectively.*

Sr No.	Site	Radius (m)	Width (m)	Wavelength (m)	Silt+Clay (%)	Age (ka)	River	Q (m^3/s) Schumm	Q (m^3/s) Carlston
1	PB	1335	272	1660	23.31	0.8 ± 0.4	HGY	736	4645
2	KY	3262	222	3850	39.54	1.5 ± 0.1	HGY	29677	28483
3	MJ	2335	476	3600	11.24	1.0 ± 0.4	HGY	1487	14449
4	KA	265	76	640	29.32	1.3 ± 0.2	ICM	70	174
5	KG	833	234	2600	65.57	1.2 ± 0.2	ICM	28094	1783
6	SV	1348	183	1900	24.33	2.5 ± 0.8	ICM	1214	4737
7	MDP	292	129	800	40.34	0.4 ± 0.1	ICM	278	212
8	SP	241	120	700	17.83	2.2 ± 0.2	ICM	30	144
9	MH	368	114	900	78.15	1.4 ± 0.1	ICM	1720	340
10	KP	976	272	2170	22.09	3.9 ± 1.4	ICM	1459	2459
11	KD	661	129	1140	28.65	2.8 ± 0.1	JMN	377	1115
12	GD	587	335	1200	13.24	3.4 ± 0.1	JMN	79	876

Sr. No.	Site	Radius (m)	Width (m)	Wavelength (m)	Silt (%)	River	Schumm Q (m^3/s)	Carlston Q (m^3/s)	Actual Discharge
1	PP	981	317	1820	67.71	HGY	10349 ± 1034	2485	7669*
2	MG	315	111	650	26.34	ICM	58 ± 6	248	54.56#
3	GD	587	335	1200	13.24	JMN	79 ± 8	876	103.64#

(HGY: Hooghly river, ICM: Icchamati river, JMN: Jamuna river)

**: Source: (Rudra, 2014)*

#: Jamuna is a tributary of tributary of Icchamati and hence the discharge should be less than the Icchamati river. (Mondal et al., 2016)

Discharge for PP is 10349 ± 1034 m^3/s (max. error) against the actual value of 7669 m^3/s (with an upper limit of 30% error) (Rudra, 2014). In contrast, Oxbow Lake MG has a calculated discharge of 58 ± 6 m^3/s (max. Error), and the documented discharge is 54.46 m^3/s. The third oxbow lake, which was GD, has a calculated discharge of 79 ± 8 m^3/s with a corresponding known value of discharge that will be less than the maximum discharge of Ichhamati River, which is 104 m^3/s.

Discharge values obtained from the formula range from a minimum of 30 m^3/s to a maximum of 29677 m^3/s **(Table 3).** Oxbow lakes with higher width and wavelength values usually show high discharge values. Oxbow lakes with a low discharge of 30, 58, 70 (all in m^3/s) are SP, MG, and KA, whereas KG obtains high discharge values, KY, PP with respective discharge as 2804, 29677, and 10349 (all in m^3/s). The discharge ranges from 30 to an average value of 1200 to 1700 m^3/s with anomalously high values up to ~28000 m^3/s. These data show that the calculated discharges based on the dimension of the meander loops are a good match and of the same order as obtained from real station data. Hence, the meander loops can be used to calculate past discharges.

4.3 OSL ages

The majority of the samples are well-bleached. Still, as far as the sensitivity of the sediments is concerned, the samples from the oxbow lakes of Jamuna and Ichhamati have better signal-to-noise ratio compared to the oxbow lakes of Hooghly **(Fig. 3)**. Point bars from Hooghly, Ichhamati and Jamuna has their sensitivities 1928 cts/Gy/mg, 4666 cts/Gy/mg, 970 cts/Gy/mg respectively. The potential for tracing sediment sources is considerable when utilizing the luminescence sensitivity of quartz. The variation in the luminescence sensitivity indicates a mix of sediment sources (Nian *et al.*, 2019) and needs separate studies to understand provenance. A high signal-to-noise ratio was observed in all the samples and thus feasible for luminescence dating. Preheat plateau and Dose recovery tests were done to check the application of the Single Aliquot Regeneration (SAR) protocol. All the ages **(Table 4)** fall well within the late Holocene period, ranging from the youngest at 0.3 ± 0.1 ka to the oldest at 3.9 ± 1.4 ka. The youngest oxbow lake at Gobardanga (GD) is at a distance of around 45 km from the presently active Hooghly River channel, and the oldest age is the oxbow lake at Beri Boar, Ramnagar (RN), located ~55 km from Hooghly River. Every point bar associated with an oxbow lake has mostly two dates, one from the bottom (sandy substrate) and one from the top. Sand layers have been dated, assuming they represent the last active flow (supported by Means size (Mz) values) in the point bar section. However, they later disconnected, shown by a silty-clayey cap representing the lake environment. Despite having a low sensitivity of ~600 cts/Gy/mg, the points bar dated in this study have some good dates for Late Holocene reconstruction. Dates

Table 4. *Luminescence Age table showing the concentration of radioactive elements (U, Th, and K), Equivalent Doses (ED), Overdispersion and Moisture content in %, and the environmental dose rate with age.*

Sr. No	Sample	Depth (cm)	U (ppm)	Th (ppm)	K (%)	Moisture (%)	Dose rate (Gy/kyr)	Aliquots	Equivalent Dose (Gy)	OD (%)	Age (ka)
1	MJ-1	15	3.3 ± 0.2	14.2 ± 0.7	2.05 ± 0.10	15	3.41 ± 0.08	28	3.4 ± 1.4	15	1.0 ± 0.4
2	MJ-2	110	3.5 ± 0.2	16.2 ± 0.8	1.67 ± 0.08	12	3.28 ± 0.09	25	1.8 ± 0.9	15	0.6 ± 0.3
3	RN-1	5	3.6 ± 0.2	10.8 ± 0.5	1.43 ± 0.07	14	2.74 ± 0.07	17	10.7 ± 3.8	20	3.9 ± 1.4
4	RN-2	45	3 ± 0.1	16.6 ± 0.8	1.43 ± 0.07	14	2.97 ± 0.08	15	8.8 ± 3.8	23	2.9 ± 1.3
5	RN-3	95	2.7 ± 0.1	16.3 ± 0.8	2.23 ± 0.11	10	3.65 ± 0.11	11	5.5 ± 1.2	26	1.5 ± 0.3
6	PB-1	15	3.2 ± 0.1	14.4 ± 0.7	1.94 ± 0.10	18	3.31 ± 0.10	19	2.7 ± 1.2	24	0.8 ± 0.4
7	PB-2	110	3.7 ± 0.2	10.1 ± 0.5	1.74 ± 0.09	14	3.05 ± 0.09	21	2.9 ± 1.6	26	0.9 ± 0.5
8	KA-1	20	3.2 ± 0.1	14.6 ± 0.7	1.99 ± 0.10	17	3.36 ± 0.10	19	4.5 ± 0.8	18	1.3 ± 0.2
9	KA-3	85	3.4 ± 0.2	15.5 ± 0.8	2.07 ± 0.10	14	3.56 ± 0.10	23	4.7 ± 0.5	21	1.3 ± 0.1
10	MDP-1	5	3.2 ± 0.1	16.3 ± 0.8	1.92 ± 0.10	15	3.40 ± 0.10	16	1.19 ± 0.2	15	0.3 ± 0.1
11	MDP-3	105	3.1 ± 0.1	15.1 ± 0.8	2.1 ± 0.11	12	3.51 ± 0.10	18	2.0 ± 0.8	18	0.6 ± 0.2
12	SV-1	25	3.1 ± 0.1	12.9 ± 0.6	2 ± 0.10	17	3.25 ± 0.09	16	8.2 ± 2.5	21	2.5 ± 0.8
13	SV-4	95	3.5 ± 0.2	18.3 ± 0.9	1.57 ± 0.08	14	3.32 ± 0.09	22	2.6 ± 0.7	24	0.8 ± 0.2
14	SP-1	20	3.3 ± 0.2	17.7 ± 0.9	1.84 ± 0.09	20	3.49 ± 0.10	20	8.0 ± 0.7	24	2.3 ± 0.2
15	SP-4	95	3.5 ± 0.2	17.9 ± 0.9	1.57 ± 0.08	15	3.25 ± 0.09	28	2.4 ± 0.3	22	0.7 ± 0.1
16	GD-2	35	3.9 ± 0.2	6.5 ± 0.3	1.7 ± 0.09	12	2.78 ± 0.08	29	9.4 ± 3.0	15	3.3 ± 0.1
17	GD-4	110	3.8 ± 0.2	13.8 ± 0.7	1.76 ± 0.09	8	3.28 ± 0.09	25	1.1 ± 0.5	14	0.3 ± 0.2
18	KG-1	0	3.6 ± 0.2	17.4 ± 0.9	1.4 ± 0.07	15	3.15 ± 0.09	17	3.8 ± 0.5	17	1.2 ± 0.2
19	KG-3	85	2.6 ± 0.1	12.4 ± 0.6	2.2 ± 0.11	12	3.29 ± 0.10	20	3.9 ± 0.6	20	1.2 ± 0.2
20	KY-2	35	2.8 ± 0.1	17.4 ± 0.9	2.3 ± 0.12	17	3.71 ± 0.11	25	5.8 ± 0.3	24	1.6 ± 0.1
21	KY-4	140	2.9 ± 0.1	15.1 ± 0.8	2.4 ± 0.12	14	3.65 ± 0.11	30	4.7 ± 0.2	25	1.3 ± 0.1
22	KD-1	5	3 ± 0.1	18.8 ± 0.9	2 ± 0.10	15	3.58 ± 0.10	19	10.0 ± 0.1	15	2.8 ± 0.1
23	KD-4	110	3.2 ± 0.1	20.2 ± 1.0	1.9 ± 0.10	12	3.61 ± 0.10	24	8.3 ± 0.7	18	2.3 ± 0.2
24	MH-1	20	2.8 ± 0.1	16.8 ± 0.8	2.4 ± 0.12	20	3.80 ± 0.11	15	5.3 ± 0.1	22	1.4 ± 0.1
25	MH-4	80	3 ± 0.1	19.3 ± 1.0	1.9 ± 0.10	16	3.50 ± 0.10	17	3.3 ± 0.2	24	0.9 ± 0.1

from Oxbow Lake Mauja (MJ) **(Fig. 5)** have shown that around 1.2 ka river was well active with trough cross-bedding at the bottom, which manifests the high discharge event exhibited by the intensification of monsoon in the Late Holocene (Gupta *et al.*, 2003). It is then followed by a ferruginous bed, which probably is a manifestation of low discharge and exposure of sediments to the atmosphere and iron precipitation due to oxygen enrichment. The sequence is followed by lamination. Then again, an active phase associated with climbing ripple marks is dated as 0.6 ka, showing the last time the river reoccupied the oxbow lake. Section from RN has channel sand age with trough cross-bedding as 3.9 ± 1.4 ka, which is again followed by a thick layer rich in ferruginous material which shows a prolonged period of aridity probably concurrent with Meghalayan Aridification; it is also mentioned as "Central Ganga plain suffers a drought phase due to possible shift in ITCZ and El Nino activity around 4.2 ka (Singh *et al.*, 2022)". The Kastadanga (KD) section has a sand bed with cross-bedding and an age of 2.8 ka (Gupta *et al.*, 2003), which suggests high discharge and matches well with a period of documented high discharge. Two dates from the KG section fall very close to each other, around 1.2 ka, despite being around 1 meter of depth difference, representing a high discharge duration in the river.

Four oxbow lakes, RN, SV, GD, and KD, have their bottom ages as 3.9 ± 1.4 ka, 2.5 ± 0.8 ka, 3.3 ± 0.1 ka, and 2.8 ± 0.1 ka, respectively (their errors are shown in age **Table 4)**. Another set of oxbow lakes, namely KY, MJ, PB, KA, and MH, has their respective channel sand ages as 1.3 ± 0.1 ka, 1.0 ± 0.4 ka, 0.8± 0.4 ka, 1.3 ± 0.2 ka, and 1.4 ± 0.1 ka.

4.4 Reccurence of high and low discharge in the study area

Size variations in the sediments can be used as a proxy for the hydrological energy of streams, sediment transport mode, and basin deposition (Weltje and Prins, 2003; 2007; Dutt *et al.*, 2018). Two significant factors mainly control the variation in grain size: i) river discharge and ii) intensity and volume of runoff, as these two factors directly affect the sediment load-carrying capacity of the river; increased coarse fraction deposition results from increased river energy and discharge, and vice versa.

The age vs. discharge graph (Ichhamati and Jamuna rivers) for our study is plotted against previously established records (see **Supplementary Figure 2**) of different proxies from Bednikund Lake (Rawat *et al.*, 2021) and Wular Lake (Lone *et al.*, 2022). Magnetic susceptibility values (Rawat *et al.*, 2021) increase during periods of solid monsoon, and most dates of channel sands from this study match well with higher magnetic susceptibility (χ) values (Rawat *et al.*, 2021), allowing us to state that point bars can be dated for monsoonal reconstruction. For Jamuna at section KD, it is observed that a ~90 cm thick silty-clayey

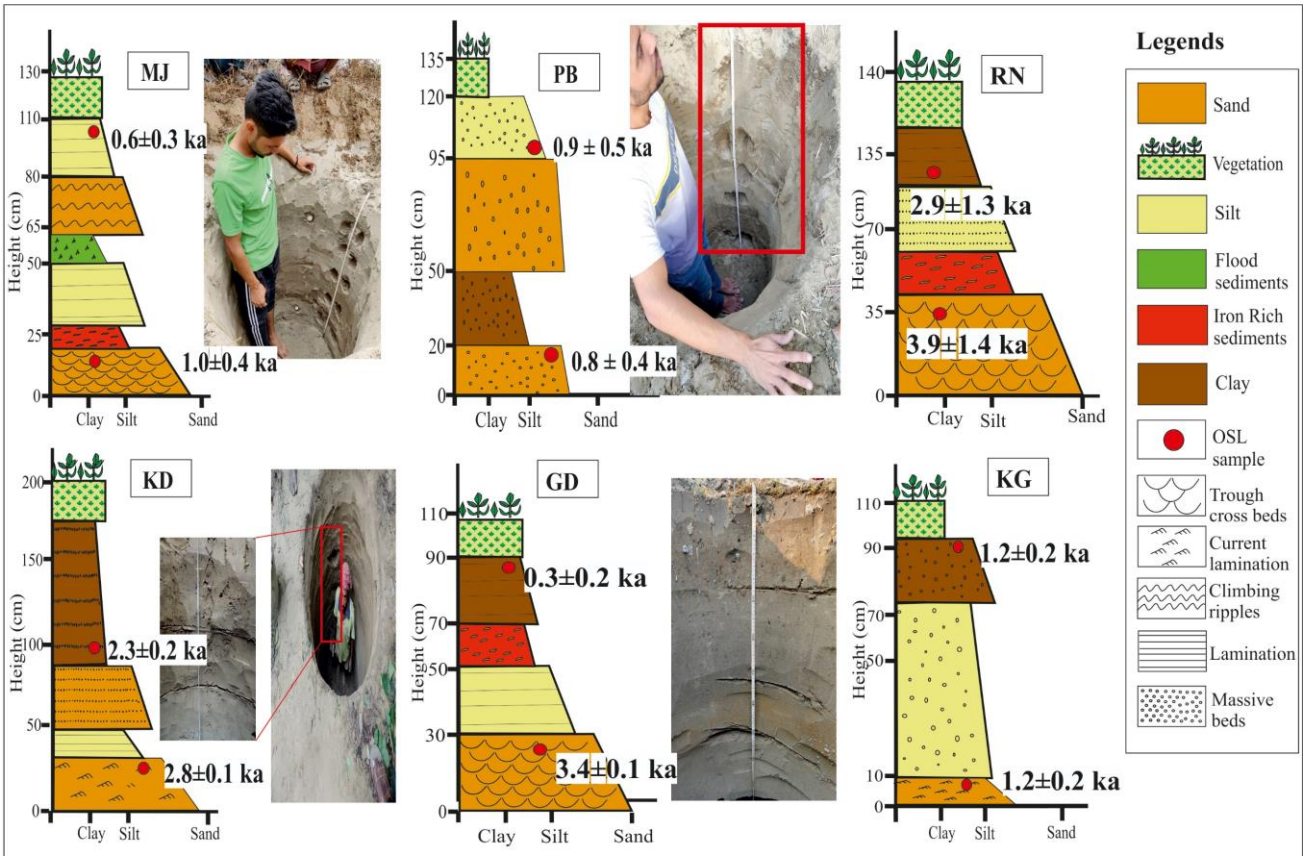

Fig. 5. *Sedimentary litho-logs the point bars along with the OSL ages.*

layer got deposited around 2.3 ± 0.2 ka, which matches with the reversal of low discharge to higher (Gupta *et al.*, 2003). For Ichhamati river, in section KG, we can see that at the very bottom, there is a coarse sand bed with a date 1.2 ± 0.2 ka that matches with a humongous discharge of 28094 m^3/s, and this is also shown in monsoon records as an intense monsoon period. For Hooghly River at section PB, major structures like trough cross beddings and cross stratifications were not found, however; medium and massive sand was found around 0.9 ± 0.5 ka that again matches both with discharge values calculated and with available monsoon records (Gupta *et al.*, 2003) **(Fig. 6)**. Ichhamati River is found to be the oldest active river among all and dates ~4 ka. Several ferruginous beds are found in Ichhamati and Jamuna, representing drier periods. Ichhamati was active till MWP, but after that dry period, no activity can be seen supported by recently calculated discharge values, and it gets considerable discharge only during floods. On the other hand, Jamuna River can be said abandoned due to Meghalayan aridification, as no coarser sediments can be found in the point bars section since, say, 2.9 ± 1.3 ka (see KD and GD in **Fig. 5**).

The results suggest a phase change of high monsoon (and thus high discharges fluvial system) during 3.9 ± 1.4 ka (1459 m^3/s) to a weakening monsoon up to 2.5 ± 0.8 ka

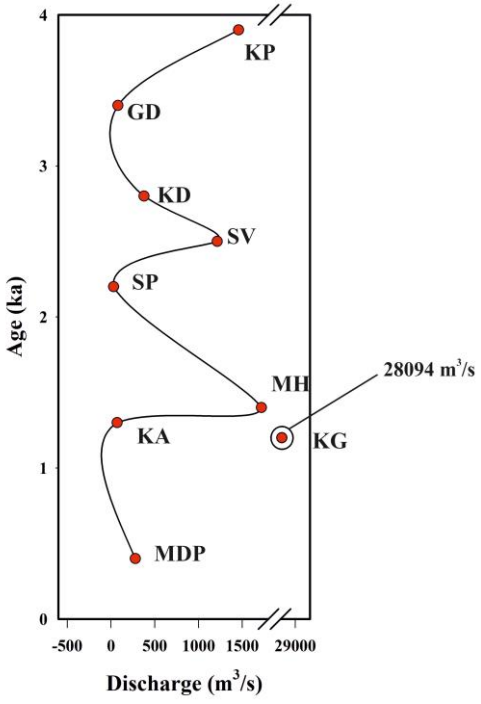

Fig. 6. *Age vs. discharge curve obtained from the discharge values from Ichhamati and Jamuna rivers.*

and then showing a strengthened monsoon, raising the discharge to a level of 1214 m^3/s **(Fig. 6)**. Another long gap of weakened monsoon followed this. Then, the rivers were all set to show the effects of the Medieval Warm period during 1.0 to 1.5 ka with highly fluctuating discharges from 30 to 28000 m^3/s, having average values of 1500 to 1700 m^3/s. This was followed by another weakening phase of monsoons that started showing from 1 ka to 800 years before and then a deficient fluvial activity during the Little Ice Age (LIA).

5. Conclusion

As suggested and inferred from the results, abandoned meander loops have the potential to contribute to reconstructing past discharges (also verified from the modern system). A few points to be concluded:

- Schumm's formula for Paleo-discharge calculation is satisfactorily applicable in the study area.
- Quartz extracted from sediments is bleached well and suitable to carry out luminescence chronology.
- Point bars can be sedimentary archives for paleo-flood and paleoclimate reconstruction.
- A discharge recurrence pattern is observed, which signifies the importance of point bars in flood frequency estimation and prediction.
- Ichhamati River seems disconnected from Ganga River during the transition from MWP to LIA, forming several paleochannels in a short duration. This suggests a high discharge condition during the transition from MWP to LIA.

Acknowledgment

I want to extend my kind gratitude to UGC for the financial assistance that made it easy to carry out this study; the authors are also grateful to the IISER Kolkata for providing all the necessities regarding field arrangement and lab accessibility.

Supplementary material

Supplementary material, containing additional figures is available online at https://doi.org/10.20858/geochr/192455.

References

Aitken MJ, 1985. Thermoluminescence dating: past progress and future trends. *Nuclear Tracks and Radiation Measurements (1982)* 10(1–2): 3–6, DOI 10.1016/0735-245X(85)90003-1.

Alam M, Alam MM, Curray JR, Chowdhury MLR and Gani MR, 2003. An overview of the sedimentary geology of the Bengal Basin in relation to the regional tectonic framework and basin-fill history. *Sedimentary geology* 155(3–4): 179–208, DOI 10.1016/S0037-0738(02)00180-X.

Baker VR, Kochel RC, Patton PC and Pickup G, 1983. Palaeohydrologic analysis of Holocene flood slack-water sediments. *Modern and ancient fluvial systems*: 229–239, DOI 10.1002/9781444303773.ch18.

Bandyopadhyay S, Kar NS, Das S and Sen J, 2014. River systems and water resources of West Bengal: a review. *Geological Society of India Special Publication*, pp. 63–84. <https://www.researchgate.net/profile/Sunando-Bandyopadhyay/publication/275833658_River_systems_and_water_resources_of_West_Bengal_A_review/links/5bf47abba6fdcc3a8de4ad49/River-systems-and-water-resources-of-West-Bengal-A-review.pdf>.

Caratini C, Bentaleb I, Fontugne M, Morzadec-Kerfourn MT, Pascal JP and Tissot C, 1994. A less humid climate since ca. 3500 yr B.P. from marine cores off Karwar, western India. *Palaeogeography, Palaeoclimatology, Palaeoecology* 109(2–4): 371–384, DOI 10.1016/0031-0182(94)90186-4.

Carlston CW, 1965. The relation of free meander geometry to stream discharge and its geomorphic implications. *American journal of science* 263(10): 864–885, DOI 10.2475/ajs.263.10.864.

Durcan JA, King GE and Duller GA, 2015. DRAC: Dose Rate and Age Calculator for trapped charge dating. *Quaternary Geochronology* 28: 54–61, DOI 10.1016/j.quageo.2015.03.012.

Dury GH, 1976. Discharge prediction, present and former, from channel dimensions. *Journal of Hydrology* 30(3): 219–245, DOI 10.1016/0022-1694(76)90102-5.

Dutt S, Gupta AK, Wünnemann B and Yan D, 2018. A long arid interlude in the Indian summer monsoon during ~4,350 to 3,450 cal. Yr BP is contemporaneous to the displacement of the Indus Valley civilization. *Quaternary International* 482: 83–92, DOI 10.1016/j.quaint.2018.04.005.

Ely LL, Enzel Y, Baker VR and Cayan DR, 1993. A 5000-year record of extreme floods and climate change in the southwestern United States. *Science* 262(5132): 410–412, DOI 10.1126/science.262.5132.410.

Folk RL and Ward WC, 1957. Brazos River bar [Texas]; a study in the significance of grain size parameters. *Journal of sedimentary research* 27(1): 3–26, DOI 10.1306/74D70646-2B21-11D7-8648000102C1865D.

Goswami K, Krishnan S, Kumerasan A, Sadasivam SK, Kumar P and Jaiswal MK, 2019. Luminescence chronology of fluvial and marine records from subsurface core in Kaveri delta, Tamil Nadu: Implications to sea level fluctuations. *Geochronometria* 46(1): 125–137, DOI 10.1515/geochr-2015-0112.

Griffiths JC, 1967. Scientific method in analysis of sediments: McGraw-Hill Book Co. *New York*, 508.

Gupta AK, Anderson DM and Overpeck JT, 2003. Abrupt changes in the Asian southwest monsoon during the Holocene and their links to the North Atlantic Ocean. *Nature* 421(6921), 354–357, DOI 10.1038/nature01340.

IMD report on Observed Rainfall Variability and Changes over West Bengal State. Met Monograph No.: ESSO/IMD/HS/Rainfall Variability/29(2020)/53

Krumbein WC, 1938. Size frequency distributions of sediments and the normal phi curve. *Journal of Sedimentary Research* 8(3): 84–90.

Lone AM, Singh SP, Shah RA, Achyuthan H, Ahmad N, Qasim A, Tripathy GR, Samanta A and Kumar P, 2022. The late Holocene hydroclimate variability in the Northwest Himalaya: sedimentary clues from the Wular Lake, Kashmir Valley. *Journal of Asian Earth Sciences* 229: 105184, DOI 10.1016/j.jseaes.2022.105184.

Maitra N, Bandopadhyay C, Samanta S, Sarkar K, Sharma AP and Manna SK, 2015. Isolation, identification and efficacy of inorganic phosphate-solubilizing bacteria from oxbow lakes of West Bengal, India. *Geomicrobiology Journal* 32(8): 751–758, DOI 10.1080/01490451.2014.981769.

Mondal I, Bandyopadhyay J and Paul AK, 2016. Estimation of hydrodynamic pattern change of Ichamati River using HEC RAS model, West Bengal, India. *Modeling Earth Systems and Environment* 2: 125, DOI 10.1007/s40808-016-0138-2.

Murray AS and Wintle AG, 2003. The single aliquot regenerative dose protocol: potential for improvements in reliability. *Radiation Measurements* 37(4–5): 377–381, DOI 10.1016/S1350-4487(03)00053-2.

Murray AS and Wintle AG, 2000. Luminescence dating of quartz using an improved single-aliquot regenerative-dose protocol. *Radiation Measurements* 32(1): 57–73, DOI 10.1016/S1350-4487(99)00253-X.

Nian X, Zhang W, Qiu F, Qin J, Wang Z, Sun Q, Chen J, Chen Z and Liu N, 2019. Luminescence characteristics of quartz from Holocene delta deposits of the Yangtze River and their provenance implications. *Quaternary Geochronology* (49): 131–137, DOI 10.1016/j.quageo.2018.04.010.

Rawat V, Rawat S, Srivastava P, Negi PS, Prakasam M and Kotlia BS, 2021. Middle Holocene Indian summer monsoon variability and its impact on cultural changes in the Indian subcontinent. *Quaternary Science Reviews* 255: 106825, DOI 10.1016/j.quascirev.2021.106825.

Rudra K, 2014. Changing river courses in the western part of the Ganga–Brahmaputra delta. *Geomorphology* 227: 87–100, DOI 10.1016/j.geomorph.2015.02.037.

Schumm SA, 1968. River adjustment to altered hydrologic regimen, Murrumbidgee River and paleochannels, Australia. US Government Printing Office, DOI 10.3133/pp598.

Singh S, Gupta AK, Rawat S, Bhaumik AK, Kumar P and Rai SK, 2022. Paleomonsoonal shifts during ~13700 to 3100 yr BP in the central Ganga Basin, India with a severe arid phase at ~4.2 ka. *Quaternary International* 629: 65–73, DOI 10.1016/j.quaint.2021.01.015.

Sridhar A, 2007. A mid–late Holocene flood record from the alluvial reach of the Mahi River, Western India. *Catena* 70(3): 330–339, DOI 10.1016/j.catena.2006.10.012.

Supriya S, 1966. Geological and geophysical studies in the western part of Bengal basin, India. *AAPG Bulletin* 50(5): 1001–1017, DOI 10.1306/5D25B60B-16C1-11D7-8645000102C1865D.

Weltje GJ and Prins MA, 2003. Muddled or mixed? Inferring palaeoclimate from size distributions of deep-sea clastics. *Sedimentary Geology* 162(1–2): 39–62, DOI 10.1016/S0037-0738(03)00235-5.

Weltje GJ and Prins MA, 2007. Genetically meaningful decomposition of grain-size distributions. *Sedimentary Geology* 202(3): 409–424, DOI 10.1016/j.sedgeo.2007.03.007.